CERTIFICATE

It is certified that the work contained in the thesis titled **"Fabrication and TCAD Simulation of TiO_2 / ZnO Nanorods Electron Transport Layer based $CH_3NH_3PbI_3$ Perovskite Solar Cell"** by **"Deepak Kumar Jarwal"** has been carried out under our supervision and that this work has not been submitted elsewhere for a degree.

It is further certified that the student has fulfilled all the requirements of Comprehensive, Candidacy and SOTA for the award of Ph. D. Degree.

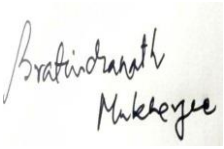

(Prof. S. Jit)
Supervisor
Department of Electronics Engineering
IIT (BHU), Varanasi

(Dr. Bratindranath Mukherjee)
Co-Supervisor
Department of Metallurgical Engineering
IIT (BHU), Varanasi

DECLARATION BY THE CANDIDATE

I, Deepak Kumar Jarwal, certify that the work embodied in this thesis is my own bonafide work and carried out by me under the supervision of Prof. Satyabrata Jit and Dr. Bratindranath Mukherjee from "21/07/2015" to “27/01/2021”, at the Department of Electronics Engineering, Indian Institute of Technology (BHU), Varanasi. The matter embodied in this thesis has not been submitted for the award of any other degree/diploma. I declare that I have faithfully acknowledged and given credits to the research workers wherever their works have been cited in my work in this thesis. I further declare that I have not will fully copied any other's work, paragraphs, text, data, results, *etc*., reported in journals, books, magazines, reports, dissertations, theses, *etc*., or available at websites and have not included them in this thesis and have not cited as my own work.

Date: 27/01/2021 **Signature of the Student**

Place: Varanasi **Deepak Kumar Jarwal**

CERTIFICATE BY THE SUPERVISOR

It is certified that the above statement made by the student is correct to the best of my knowledge.

(Prof. S. Jit)
Supervisor
Department of Electronics Engineering
IIT (BHU), Varanasi

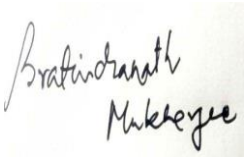

(Dr. Bratindranath Mukherjee)
Co-Supervisor
Department of Metallurgical Engineering
IIT (BHU), Varanasi

Signature of Head of Department
"SEAL OF THE DEPARTMENT"

COPYRIGHT TRANSFER CERTIFICATE

Title of the Thesis: **Fabrication and TCAD Simulation of TiO_2 / ZnO Nanorods Electron Transport Layer based $CH_3NH_3PbI_3$ Perovskite Solar Cell**

Name of the Student: **Deepak Kumar Jarwal**

Copyright Transfer

The undersigned hereby assigns to the Indian Institute of Technology (Banaras Hindu University), Varanasi all rights under copyright that may exist in and for the above thesis submitted for the award of the Doctor of Philosophy.

Date: 27/01/2021 **Signature of the Student**

Place: Varanasi **Deepak Kumar Jarwal**

Note: However, the author may reproduce or authorize others to reproduce material extracted verbatim from the thesis or derivative of the thesis for author's personal use provided that the source and the Institute's copyright notice are indicated.

ACKNOWLEDGEMENT

First and foremost, I want to dedicate my honest prayer to Pujya Gurudev who has given me the strength, knowledge, ability and opportunity to undertake this research study and to complete it satisfactorily. I am humbled and exceedingly joyful as a witness to his countless blessings.

First of all, I would like to express my immense gratitude and sincere thanks to my supervisor Prof. Satyabrata Jit and Co-supervisor Dr. Bratindranath Mukherjee for their continuous support, motivation and valuable guidance. Their immense knowledge and guidance helped me a lot to carry out my research work. Without their precious and whole hearted support the successful completion of this research work would have not been possible. The insightful discussions with them always provided me great enthusiasm.

I wish to extend my sincere gratitude towards my research programme committee (RPC) members Prof. V. N. Mishra, Dr. Bholanath Pal, and all the Departmental Research Committee (DRC) members for their valuable suggestions and fruitful discussions during the entire period of my research. A vote of thanks from the bottom of my heart goes to the Head of Electronics Engineering Department, IIT (BHU), Varanasi for providing me all of the necessary tools and lab facilities to conduct my research work. I would also like to thank all the faculty members, laboratory staff, librarians and office staff for their kind cooperation and encouragement during this journey.

My thanks and deep appreciations also go to all staff members of CRME lab, Department of Electronics Engineering, especially to Mr. M. K. Saxena, Mr. S. C. Yadav, Mr. Sanjeev Srivastava, Mr. Shyam Narayan, and Mr. Vinay Srivastava for their kind co-operation.

I would like to express my special thanks to my seniors Dr. Gopal Rwat, Dr. Hemant Kumar Bhatt, Dr. Yogesh Kumar, Dr. Chandan Kumar, Dr. Kunal Singh, Dr. Sanjay Kumar, Dr. Balraj Singh, Dr. Sweta Chander, Dr. Ekta Goyal, Mr. Lalit Chandra, Mr. P. K. Sahu, Dr. Subhiman Chatterjee, Dr. Gaorav Modanwal for their constant encouragement and suggestions.

I have great pleasure in acknowledging my colleagues and fellow Mr. Kamlaksha Baral, Mr. Ashwini Kumar Mishra, Mr. Amit Kumar, Mr. Smriti Ratan, Mr. Prince Kumar Singh, Mr. Rishibrind Upadyay, Mr. Abhinav Pratap Singh, Mr. Deepchand Upadyay, Mr. Abhisekh Kumar, Mr. Ashutosh Dixit, Mr. Jogendra Singh Rana, Mrs Sikha Singh for their motivation, support, and encouragement. I wish to extend my special thanks to all of them for providing a nice, friendly and peaceful research environment.

I am very much thankful to many research scholars Mr. Prabhakar Tripathy, Mr.Akash Prajapati, Mr. Vinit Singh, Mr. Mumtaj Ali Ansari, Mr. Aman Sikri, Mr. Rahul Pal, and Mr. Arjun Yadav for their fruitful suggestions.

My thanks and sincere appreciations also go to my friend, especially to Mr. Sunil Kumar, Mr. Amit Kumar Soni, Mr. Kaushal Kishor Gupta and Mr. Yash Sukla for their constant support.

I would like to express my heart-felt gratitude to my beloved parents Shri. Ramswaroop Jangid and Smt. Shushila Devi for their constant support and love throughout my life. I am always indebted to my grandparents for their eternal blessings.

At this very special moment, however no words will be enough but I heartily express sincere thanks to my sisters Mrs. Archana Jangir and Dr. Nisha Jarwal. They are the source of moral and emotional strength in my life. I have a sincere appreciation for my sister in law Mrs. Anjali Baberwal for giving us sparkles like Aayush Jarwal and Aayan Jarwal.

My most profound appreciation towards my brothers Mr. Arvind Jarwal and Mr. Vikash Jarwal for their continuous support and encouragement. They are the source of strength and remain an invaluable asset to me.

It is a privilege to express my sincere regards and love for my fiancé Miss Deepika Jangid for her constant support, unconditional love, faith, and encouragement.

Finally, I heartily express sincere thanks to my Jarwal family and especially to Mr. Jitendra Kumar Jangir for their extreme patience and constant support over the years. They provided me strength and confidence to attain this task.

Above all, I thank Lord Vishwanath for providing me strength and courage in completing the work.

Date: 27/01/2021 ***(Deepak Kumar Jarwal)***

DEDICATED TO MY BELOVED

PUJYA GURUDEV

CONTENTS

List of Figures x-xiv

List of Tables xv

List of Abbreviations xvi-xviii

List of Symbols xix-xxi

Preface xxii-xxvi

CHAPTER 1 **1-46**

Introduction and Scope of the Thesis

1.1 Solar Cell 3

1.1.1 Origin of Solar Cells 4

1.1.2 Generation of Solar Cells 5

1.2 Perovskite Solar Cell 8

1.2.1 Perovskite Material 9

1.2.1.1 Crystal Structure 10

1.2.1.2 Optoelectronic Properties 11

1.2.2 Working Principle of Perovskite Solar Cells 13

1.2.3 Numerical Modeling of Perovskite Solar Cells 17

1.3 Fabrication Process for Perovskite Solar Cells 21

1.3.1 Electrodes 22

1.3.2 Photoabsorber Layers 23

1.3.2.1 One Step Deposition via Spin Coating 24

1.3.2.2 Two Step Deposition via Spin Coating 25

1.3.2.3 Vapor Assisted Deposition Technique 26

1.3.3 Charge Transport Layers 26

1.4 Characterization Techniques for Perovskite Solar Cells 29

1.4.1 Surface Characterization 29
1.4.1.1 Atomic Force Microscopy 29
1.4.1.2 Scanning Electron Microscopy 30
1.4.1.3 Transmission Electron Microscopy 30
1.4.1.4 X-Ray Diffraction 31
1.4.2 Optical Characterizations 32
1.4.2.1 Absorbance 32
1.4.2.2 Photoluminescence 32
1.4.3 Optoelectronic Characterizations 33
1.5 Literature Review 35
1.5.1 Review of Perovskite Based Solar Cells 35
1.5.2 Review of TiO_2 Nanorods Based Perovskite Solar Cells 38
1.5.3 Review of ZnO Nanorod Based Perovskite Solar Cells 39
1.5.4 Major Observation from the Literature Survey 41
1.6 Issues and Challenges in Perovskite Solar Cells 42
1.7 Motivation and Problem Definition 43
1.8 Scope of the Thesis 44

CHAPTER 2 47-63

Effect of TiO_2 Nanorods (TNRs) ETL Thickness on the Performance of FTO/TNRs/$CH_3NH_3PbI_3$/PTAA/Pd Structure Based Perovskite Solar Cells

2.1 Introduction 48
2.2 Experimental Details 50
2.2.1 Material Used 50
2.2.2 TiO_2 Nanorods Synthesis and $TiCl_4$ treatment 50
2.2.3 CH_3NH_3I Perovskite Precursor Synthesis 51
2.2.4 Device Fabrication 51

2.3	Numerical Modeling and Device Simulation		52
2.4	Results and Discussion		56
	2.4.1	Thin Film Characterization	56
	2.4.2	Solar Cell Characterization	58
2.5	Conclusion		62

CHAPTER 3 **64-84**

Effects of Solvothermal Etching and $TiCl_4$ Treatment of TiO_2 Nanorods (TNRs) ETL on the Performance Characteristics of FTO/TNRs/$CH_3NH_3PbI_3$/Spiro-OMeTAD/Pd Solar Cells

3.1	Introduction		65
3.2	Experimental Details		66
	3.2.1	Preparation of Electron Transport Layer (ETL)	66
	3.2.2	Solar Cell Fabrication	69
	3.2.3	Material and Device Characterization	70
3.3	Results and Discussion		72
	3.3.1	Thin Film Characterization	73
	3.3.2	Solar Cell Characterization	79
3.4	Conclusion		83

CHAPTER 4 **85-102**

Fabrication and Characterization of FTO/ZnO Seed Layer/ZnO Nanorods/$CH_3NH_3PbI_3$/PTAA/Au Solar Cells with Different Seed Layers

4.1	Introduction		86
4.2	Experimental Details		87
	4.2.1	Solution Preparation for Seed Layer	87
	4.2.2	Growth of ZnO Nanorods	89

	4.2.3	Solar Cell Fabrication	91
4.3	Results and Discussion		92
	4.3.1	Thin Film Surface Characteristic	93
	4.3.2	Optical Characterization	95
	4.3.3	Electrical Characterization	98
4.4	Conclusion		102

CHAPTER 5 **103-119**

Effect of Doped Spiro-OMeTAD Based HTL on the Performance of FTO/ZnO Nanorods/$CH_3NH_3PbI_3$/ Spiro-OMeTAD/Pd Perovskite Solar Cells

5.1	Introduction		104
5.2	Experimental Details		105
	5.2.1	Thin Film Growth and Perovskite Solar Cell Fabrication	105
	5.2.2	Film and Device Characterization	107
5.3	TCAD Simulation and Models		108
5.4	Results and Discussion		110
	5.4.1	Thin Film Characterization	111
	5.4.2	Solar Cell Characterization	114
5.5	Conclusion		119

CHAPTER 6 **120-127**

Conclusion and Future Scope

6.1	Introduction	121
6.2	Chapter-Wise Major Observations	122
6.3	Future Scope of Work	126

References **128-147**

Author's Relevant Publications **148-149**

LIST OF FIGURES

Figure 1.1:	Various non-renewable and renewable energy sources.	**4**
Figure 1.2:	Different generations of solar cells.	**7**
Figure 1.3:	Comparative rapid growth in PCE for perovskite based solar cells.	**8**
Figure 1.4:	(a) Structure of ABX_3 perovskite (b) Cubic unit cell of $CH_3NH_3PbI_3$.	**11**
Figure 1.5:	Band structure of $MAPbI_3$.	**12**
Figure 1.6:	General structure of perovskite solar cell.	**14**
Figure 1.7:	Electrical equivalent model of the perovskite solar cell.	**15**
Figure 1.8:	J-V curve for PSC device where the red curve is for under illumination and black is for dark. The area in the shade gives maximum achievable power.	**16**
Figure 1.9:	Band-to-band, SRH, and Auger recombination.	**21**
Figure 1.10:	Block diagram of physical vapor deposition.	**22**
Figure 1.11:	Deposition methods for the perovskite thin film (a) Physical vapor deposition, (b) One step deposition, and (c) Two step deposition.	**24**
Figure 1.12:	Measurement setup for (a) AFM, (b) HRSEM, (c) TEM, and	**31**

(d) XRD.

Figure 1.13: Measurement setup for (a) Photoluminescence spectrometer and (b) UV-Vis absorption spectroscopy. **33**

Figure 1.14: Optoelectronic characterization setup for perovskite solar cells. **34**

Figure 1.15: Progress in power conversion efficiency of PSCs from 2005 to 2018. **36**

Figure 2.1: (a) Device structure of the PSCs. (b) Band diagram for the fabricated PSCs structure under equilibrium. **52**

Figure 2.2: (a) Equivalent circuit of perovskite solar cell; (b) Equivalent *J-V* characteristic and performance parameters of PSC. **52**

Figure 2.3: (a) HRSEM image of TNRs and (b) EDS image of TNRs. **57**

Figure 2.4: (a) XRD pattern of hydrothermally synthesized TNRs and (b) PL emission spectra of perovskite thin film. **57**

Figure 2.5: HRSEM image of (a) perovskite thin film surface (b) Cross-sectional view of PSC structure without metal electrode. **58**

Figure 2.6: (a) Absorbance spectra of hydrothermally synthesized and simulated TNRs on FTO coated glass substrate, (b) Absorbance spectra of synthesized and simulated perovskite thin film. **58**

Figure 2.7: J-V curve of fabricated and simulated PSCs with (a) 500 nm TNRs, (b) 650 nm TNRs, (c) 800 nm TNR **60**

Figure 2.8: External quantum efficiency of fabricated and simulated PSCs with 500 nm ETL, 350 nm active layer and 100 nm HTL. **62**

Figure 3.1: (a) FTO coated glass, (b) TiO_2 seed layer on FTO coated glass, (c) Hydrothermal Process at 170^0C in Teflon lined cylinder, (d) TNRs after hydrothermal process, (e) Solvothermal etching of **68**

TNRs at 180^0 C and (f) TiO_2 NRs after solvothermal etching.

Figure 3.2: Fabrication steps used for device A, B and C. **71**

Figure 3.3: (a) The device structure of PSC after solvothermal etching of TiO_2 NRs and (b) Schematic representation of the energy band diagram of PSC. **72**

Figure 3.4: (a) XRD analysis of TiO_2 NRs annealed at 450^0 C. (b) Energy dispersive spectroscopy (EDS) and elemental composition of TNRs. **74**

Figure 3.5: (a) And (c) are the TEM images of pristine rutile TNRs and TNRs after solvothermal etching respectively. Fig. (b) and (d) are the selected area electron diffraction patterns corresponds to Fig (a) and (b) respectively. **75**

Figure 3.6: Top view SEM image of TNRs annealed at 450^0 C in ambient environment before solvothermal etching: (a) 200 nm scale, (b) 500 nm scale (Inset of Figure 3.6 (b) shows the cross-sectional image of TNRs at 500 nm scale); after solvothermal etching: (c) 200 nm scale, (d) 500 nm scale. Top SEM image of perovskite thin film deposited on solvothermal etched TNRs (e) 200 nm scale and (f) 500 nm scale. **76**

Figure 3.7: AFM image of TNRs without solvothermal etching (a) 2D and (b) 3D. AFM image of TNRs with solvothermal etching (c) 2D and (d) 3D. AFM image of perovskite film deposited on etched TNRs (e) 2D and (f) 3D. **77**

Figure 3.8: (a) Transmittance of TiO_2 NRs before and after solvothermal etching. (b) UV-VIS absorbance spectrum of perovskite film deposited on TiO_2 nanorods without $TiCl_4$ treatment, TiO_2 nanorods with $TiCl_4$ treatment before and after solvothermal etching. **79**

Figure 3.9:	(a) *I-V* characteristics of the junction diode made of modified TNRs. Inset of (a) shows SCLC region in all the diode. (b) Emission characteristics in three solar cell structures of TiO_2 NRs before and after solvothermal etching. Inset of (b) shows impedance characteristics of three solar cells.	**82**
Figure 3.10:	(a) J_{ph}-V characteristics of Device A, B and C. (b) Comparison of EQE of Device A, B and C.	**83**
Figure 4.1:	Graphical view of the preparation process of the solutions for the seed layers (a) ZnO drop-cast (b) ZnO NPs (c) ZnO QDs (d) Solvothermal ZnO NRs.	**88**
Figure 4.2:	Seed layer deposition process using drop-cast, spin coating, and solvothermal. Growth of nanorods in the last step using the solvothermal process.	**90**
Figure 4.3:	Fabrication flow diagram for the perovskite solar cell.	**92**
Figure 4.4:	Top view of ZnO nanorods grown on different seed layers of (a) drop-cast (b) spin coated (ZnO NPs) (c) spin coated (ZnO QD) (d) solvothermal.	**94**
Figure 4.5:	XRD pattern of ZnO NR grows on different ZnO seed layers deposited using (a) drop-cast (b) spin coated (ZnO NPs) (c) spin coated (ZnO QD) (d) solvothermal.	**95**
Figure 4.6:	Photoluminescence emission and optical absorbance spectra of ZnO seed layer samples deposited on FTO substrate.	**96**
Figure 4.7:	Tau plots for different ZnO seed layer samples.	**97**
Figure 4.8:	Transmittance spectra of ZnO nanorods deposited on various ZnO seed layer.	**100**
Figure 4.9:	Impedance characteristics of PSCs A, B, C, & D	**100**

Figure 4.10:	Current density vs voltage (J-V) curve of four ZNRs based PSCs Fabricated on different ZnO seed layers.	**101**
Figure 4.11:	External quantum efficiency (EQE) of PSCs A, B, C, and D	**102**
Figure 5.1:	(a)Fabrication flowchart for the PSCs. (b) Complete device structure of the fabricated PSCs.	**107**
Figure 5.2:	(a) Energy band diagram of perovskite solar cell and (b) Equivalent electrical circuit.	**109**
Figure 5.3:	(a) Transmitance spectra of ZnO NRs and (b) Tauc plot for ZnO NRs.	**112**
Figure 5.4:	AFM image of (a) ZnO NRs without $TiCl_4$ treated, (b) ZnO NRs with $TiCl_4$ treatment, and (c) Perovskite layer on ZnO NRs	**113**
Figure 5.5:	HRSEM image of (a) ZnO quantum dot, (b) Solvothermally synthesized ZnO NRs, (b) Perovskite thin film on ZnO NRs, and (d) Cross-sectional image of perovskite layer on ZnO NRs.	**114**
Figure 5.6:	(a) Nyquist plot for fabricated PSC with undoped and doped HTL layer; (b) Equivalent circuit model employed using impedance characteristics.	**116**
Figure 5.7:	(a) Imaginary impedance vs. frequency plot, and (b) Real impedance vs. frequency plot of fabricated PSCs	**116**
Figure 5.8:	Current density vs. voltage curve for (a) Undoped spiro-OMeTAD and (b) Doped spiro-OMeTAD.	**117**
Figure 5.9:	External quantum efficiency of (a) Undoped spiro-OMeTAD based PSC and (b) Doped spiro-OMeTAD based PSC.	**118**

LIST OF TABLES

Table 1.1:	Comparison of optical properties of perovskite with other materials.	**10**
Table 1.2:	Comparison of different deposition techniques for charge transport layers.	**28**
Table 2.1:	The Material Parameters for Numerical Simulation.	**55**
Table 2.2:	Fabricated and Simulated Results for Different ETL of the PSCs	**61**
Table 3.1:	Device comparison based on TiO_2 NRs ETL.	**82**
Table 3.2:	Power conversion efficiency of TiO_2 ETL based PSCs.	**83**
Table 4.1:	Photovoltaic parameter of different PSCs based on different seed layers.	**99**
Table 5.1:	Different parameters used in the simulation of PSCs.	**109**
Table 5.2:	A comparison of fabricated and simulated PSC parameters.	**118**

LIST OF ABBREVIATIONS

Abbreviation	Details
PV	Photovoltaic
LED	Light Emitting Diode
P3HT	Poly(3-hexylthiophene)
HOMO	Highest Occupied Molecular Orbital
LUMO	Lowest Unoccupied Molecular Orbital
PEDOT	Poly(3,4-ethylenedioxythiophene)
PCE	Power Conversion Efficiency
AM	Atmospheric Mass
SPM	Scanning Probe Microscopy
AFM	Atomic Force Microscopy
STM	Scanning Tunnelling Microscopy
GaAs	Gallium Arsenide
HRSEM	High Resolution Scanning electron microscopy
EDX or EDS	Energy dispersive X-ray spectroscopy
TEM	Transmission Electron Microscopy
SAED	Selected Area Electron Diffraction
XRD	X-ray Diffraction
CIGS	Copper Indium Gallium Selenide
UV-Vis	Ultraviolet-Visible
PL	Photoluminescence
ZnO	Zinc Oxide
PET	Polyethylene Terephthalate
CdTe	Cadmium Telluride
CdS	Cadmium Sulphide
TiO_2	Titanium dioxide

Au	Gold
Ag	Silver
Al	Aluminum
MoO_3	Molybdenum Trioxide
RMS	Root Mean Square
ITO	Indium-Doped Tin Oxide
FTO	Fluorine Doped Tin Oxide
TCAD	Technology Computer Aided Design
EPBT	Energy Pay Back Time
PCBM	[6,6]-phenyl C_{61} butyric acid methyl ester
QDs	Quantum Dots
DSSCs	Dyed Sensitized Solar Cells
PSC	Perovskite Solar Cell
ETLs	Electron Transport Layers
HTLs	Hole Transport Layers
$MAPbX_3$	Methyl Ammonium Lead Halides
$CsPbX_3$	Caesium based Lead Halides (Cl, Br, I)
VB	Valence Band
CB	Conduction Band
Pb	Lead
eV	Electron Volt
PTAA	Poly(triaryl amine)
TCO	Transparent Conducting Oxide
FF	Fill Factor
SRH	Shockley Read Hall
PVD	Physical Vapour Deposition
DMF	Di-Methyl Formamide
DMSO	Di-Methyl Sulfoxide

GBL	g-Butyro- Lactone
NMP	N-Methyl-2-Pyrrolidone
Al_2O_3	Aluminium Oxide
PECVD	Plasma Enhanced Chemical Vapor Deposition
CBD	Chemical Bath Deposition
AC	Alternating Current
P3HT	Poly(3-Hexylthiophene)
CuSCN	Copper(I) thiocyanate
HTM	Hole Transport Material
ETM	Electron Transport Material
ZNRs	ZnO Nanorods
C_{60}	Fullerenes
PCBM	Phenyl-C61-butyric acid methyl ester
TNRs	TiO_2 Nanorods
ZrO_2	Zirconium dioxide
SnO_2	Tin(IV) oxide
ALD	Atomic Layer Deposition
$TiCl_4$	Titanium Tetrachloride
TTIP	Titanium Iso-propoxide
HI	Hydrogen Iodide
RPM	Rotation Per Minute
DOS	Density of State

LIST OF SYMBOLS

Symbol	Details
λ	Wavelength
θ	Diffraction angle
T	Transmittance
A	Absorbance
I-V	Current-voltage
CV	Capacitance-voltage
μ_e	Electron mobility
μ_h	Hole mobility
V_T	Thermal voltage
I_{SH}	Current through Shunt resistance
I_{PH}	Photo generated current
I	Current
I_S	Reverse Saturation Current
B	Ratio of photo-generated current to the light intensity
N_t	Defect Density
N_A	Doping concentration of Acceptor
N_D	Doping concentration of Donor
P	Power Density
R_S	Series Resistance
E_G	Energy Band Gap
R_{SH}	Shunt Resistance
FF	Fill Factor

J_{SC}	Short Circuit Current density
η	Power Conversion Efficiency
J	Current Density
V	Voltage
X	Electron Affinity
N_C	Density of states of the Conduction Band
N_V	Density of states of the Valence Band
$h\upsilon$	Photon Energy
P_T	Theoretical Power
I_{sc}	Short Circuit Current
P_{in}	Incident Optical Power Density
P_{mpp}	Maximum Power Density
J_{mpp}	Maximum Current Density
V_{mpp}	Maximum Voltage
V_{OC}	Open Circuit Voltage
n	Concentration of Electrons
p	Concentration of Holes
R	Recombination Rate
G	Generation Rate
γ	Recombination Coefficient
n_i	Intrinsic Carrier Concentration
R_{SRH}	Rate of SRH combination
V	Voltage
τn	Electron Lifetime
τp	Hole Lifetime
E_C	Energy of Conduction band
E_V	Energy of valence band

keV	Kilo Electron Volt
C	Capacitance
$C_p{}^A$	Constant
$C_n{}^A$	Constant
V	Voltage
ε_o	Vacuum Permittivity
ε_r	Relative Permittivity
$\Phi(x)$	Electrostatic Potential
e	Electric Charge
J_n	Current Density due to Electrons
J_p	Current Density due to Holes
ρ_d	Defect Charge Density

PREFACE

The worldwide increase in energy consumption has motivated scientists to explore the potential of solar energy. At present, solar energy harvesting is carried out mostly (more than 90%) by the inorganic crystalline silicon (Si) solar cells. Moreover, Si-based solar cells are now approaching their maximum theoretical limiting efficiency of ~29.43%. The latest advancements in technology and materials have led to the development of novel photosensitive materials that enabled the fabrication of low cost and highly efficient photovoltaic devices. The state of the art growth in various perovskite materials like inorganic ($CsPbX_3$: X=I, Cl, Br) and hybrid (ABX_3; A= organic compound, B= inorganic compound, and X= halides) have attracted huge interest among the researchers. Recently, methylammonium lead halides ($CH_3NH_3PbX_3$) have shown highly encouraging photosensitive for photovoltaic application, which gained immense research attention since its discovery and has boosted hopes for new photovoltaic technologies.

Typically, the optical and electrical characteristics of photovoltaic devices depend upon the device design, fabrication procedures, semiconductor/active material, etc. The different synthesis and deposition techniques may be used for the tuning of the electronic and optical properties of as-grown thin films. Additionally, the low-dimension nanostructures such as nanorods or nanowires that offer large surface-to-volume ratios are mostly used for the charge transport layer in perovskite solar cells (PSC). From this perspective, the present thesis deals with the TCAD simulation, fabrication, and characterization of TiO_2/ZnO nanorods electron transport layer (ETL)

based hybrid perovskite ($CH_3NH_3PbI_3$) solar cells. In PSCs' design, the PTAA/Spiro-OMeTAD polymer is employed as hole transport material where small molecule materials (Li-TFSI and TBP) are used as doping elements to enhance the conductivity of the hole transport layer (HTL).

The primary focus of this thesis is to explore the performance parameter of PSC by means of the synergic effects of the modified synthesis process for ETL through optimized doping in HTL. The uniformly distributed and vertically aligned TiO_2/ZnO Nanorods have been grown on FTO substrates by the hydrothermal method, whereas both HTL and absorber layers are deposited via spin-coating techniques. Later, the optical and electrical properties of TiO_2/ZnO Nanorods have been explored in detail. The thesis consists of six chapters, which are briefly outlined as follows:

Chapter-1 introduces the hybrid perovskite material's optoelectronic properties, thin-film synthesis process, and the working principle of perovskite solar cells. A brief introduction about device models and thin film characterization techniques have been discussed. Finally, a detailed literature survey, motivation, and scope of the thesis have been presented.

Chapter-2 presents TCAD simulation and fabrication of hybrid perovskite solar cells. The electrical and optical characterization has been investigated for the device structure Pd/PTAA/hybrid perovskite ($CH_3NH_3PbI_3$)/TiO_2 Nanorods (TNRs) grown on an FTO coated glass substrate. The TNRs layer is synthesized by a low-cost hydrothermal process and acts as the ETL, whereas the PTAA acts as the HTL. The solar cells are optimized, fabricated, and characterized for different TNRs thickness and then several device performance parameters such as short circuit current density (J_{SC}),

open-circuit voltage (V_{OC}), fill factor (*FF*), and power conversion efficiency (*PCE*) and etc. are studied. The *Solar Cell Capacitance Simulator-One Dimensional* (SCAPS-1D) is used to simulate the proposed solar cell structure and validated via our experimental results. The effects of thickness variation of ETL on the solar cell parameters have been investigated by solving the drift-diffusion model. The measurements show that the efficiency of the solar cell is decreased with the increase in ETL thickness, which is attributed to higher trap sites in the active layer and ETL. The maximum optimized efficiency of 15.04% is obtained for ETL thickness of 500 nm. On the other hand, the simulated results are in close resemblance to the experimental results, having an efficiency of 15.69%.

Chapter-3 reports the efficiency improvement of perovskite solar cells (PSCs) by solvothermal etching and $TiCl_4$ treatment of TNRs based ETL. The TiO_2 NRAs have been explored for the ETL due to their better direct carrier transportation over other TiO_2 nanostructures. The solvothermal etching of TiO_2 NRAs enhances the surface-to-volume ratio of the ETL, which, in turn, enhances the power conversion efficiency (PCE) of the PSCs. All the measurements have been performed at room temperature and high humid (with ~65% humidity) conditions to demonstrate the performance of the PSCs under normal environmental conditions. A noteworthy efficiency of 15.16% with an improved fill factor (FF) and short circuit current density (J_{SC}) has been reported in the proposed PSCs. The PSC performance is further improved by the $TiCl_4$ treatment of the solvothermally etched TiO_2 NRs as the ETL in the device.

Chapter-4 discusses the effect of the seed layer, which directly affects the growth of the ZnO Nanorods (ZNRs) and related photovoltaic parameters of the hybrid

perovskite solar cell. Four different types of ZnO seed layer samples have been synthesized using four methods, namely: ZnO drop-cast, ZnO nanoparticles (NPs), ZnO quantum dots (QDs), and ZnO solvothermal on the FTO substrate. ZnO drop-cast results in less density, tilted, and non-uniform deposition of the nanorods. But uniform coverage, high volume to the surface, and vertical direction growth of ZNRs are observed in the ZnO QD seed layer sample compared to the other three samples. Morphology and crystalline structure were analyzed with HRSEM, TEM, and XRD, whereas optical absorption, emission, and transmittance are recorded using UV-Visible, and Photoluminescence, respectively. Subsequently, the electrical characterization reveals that the optimum photovoltaic parameters are obtained on the seed layer of ZnO QD, which leads to the power conversion efficiency of 10.69% for ZnO NR based perovskite solar cell structure (FTO/ZNRS/$CH_3NH_3PbI_3$/PTAA/Au).

Chapter-5 presents the simulation, fabrication, and characterization of ZnO Nanorod (ZNRs) based PSCs under ambient air conditions. The proposed PSC structures use a $CH_3NH_3PbI_3$ hybrid perovskite-based active layer sandwiched between a ZnO Nanorods (NRs) ETL and a Spiro-OMeTAD (undoped and doped) HTL. The ZnO NRs are grown using a low-cost solvothermal process at relatively low temperature. The performance of fabricated PSCs is analyzed for both the undoped and doped (with TBP and LiTFSI) spiro-OMeTAD based HTLs. All the solar parameters, namely, short circuit current density (J_{SC}), open-circuit voltage (V_{OC}), fill factor (*FF*), power conversion efficiency (*PCE*), and external quantum efficiency (*EQE*), are calculated from experimentally measured current density versus voltage (*J-V*) and wavelength transient characteristics in ambient condition. The maximum *PCE* of 10.18% is obtained for the doped HTL, whereas 9.51% for undoped HTL. The

improved performance due to HTL doping is attributed to the enhanced charge transportation of the HTL. The experimental results obtained from the fabricated PSCs are also compared with the SetFos^{TM} TCAD simulation data using the drift-diffusion model. The simulated results are observed to be well matched to the experimental data.

Chapter-6 includes the major findings of the thesis along with a brief outline for the future scope of research related to the present thesis.

----XXX----